



# Stress–strain–strength behavior of geosynthetic reinforced rubber–sand mixtures

Mengtao Wu<sup>1,2</sup> · Fangcheng Liu<sup>1</sup> · Jun Yang<sup>2</sup>

Received: 7 July 2022 / Accepted: 13 March 2023

© The Author(s), under exclusive licence to Springer-Verlag GmbH Germany, part of Springer Nature 2023

## Abstract

As a lightweight and energy-dissipating filler, rubber-sand mixture (RSM) is promising for a wide range of applications in civil engineering. However, the shear strength of RSM decreases with higher rubber content compared to that of sandy soil alone. To overcome this issue, geosynthetics are placed within RSM to increase the shear strength and overall stability of the system. This paper focuses on the stress–strain–strength behavior of geogrid-reinforced RSM, with the aim of expanding the application of RSM in geotechnical, traffic and seismic fields. Based on triaxial compression tests, the stress–strain response and strength parameters of geogrid-reinforced RSM considering the effects of reinforcement layers, rubber contents and confining pressures were analyzed. The test results indicate that the strength parameters of the geogrid-reinforced RSM are significantly improved compared to the unreinforced case, and the incremental amplitude increases with increasing the number of reinforcement layers and decreasing the confining pressure. The reinforced RSM with a 20% rubber content (by weight) might be the optimum for the use of reinforcement with geosynthetics. Additionally, a new equation is proposed to estimate the strength reinforcement effect of the composite mixtures, which could provide a reference for subsequent theoretical research and engineering applications.

**Keywords** Geosynthetics · Rubber–sand mixtures · Shear strength · Stress–strain relationship

## 1 Introduction

Rubber–sand mixture (RSM) is made of waste tire rubber (e.g., granulated rubber, tire chips and tire shreds) and sandy soil. Owing to its characteristics of light weight, strong elastic deformation ability, low shear modulus and large damping, RSM can be widely used in various engineering projects. For instance, it has been used as a light filler for abutment and retaining walls [46, 53], for soft foundation treatment [41, 49], for pipeline backfilling

[9, 38, 50], for road and slope construction [39, 64], and as a natural base isolator for earthquake protection [44, 52, 58]. From an environmental perspective, the safe and beneficial use of tire rubber overcomes the issues associated with waste tire treatment and provides long-term safety. Laboratory tests and field studies have demonstrated that there is little or no significant leaching of those substances of specific public health concern from tire chips, which proves that recycled scrap tires are not hazardous materials [11, 34, 52]. Additionally, as a hydrophobic material, rubber has almost no reaction with underground water, and the adverse environmental impact on soil and groundwater is minor. Consequently, RSM is an eco-friendly engineering material that provides a sustainable solution to various projects.

Since the 1990s, the mechanical properties of the mixtures of tire chips/scrap rubber and sand/soil have been studied, and many valuable conclusions have been made. Ahmed et al. [1] carried out triaxial tests on tire chip-sand mixtures. Their results showed that the shear performance of the mixture depends on the specimen preparation

✉ Fangcheng Liu  
fcliu@hut.edu.cn

Mengtao Wu  
cewu@hku.hk

Jun Yang  
junyang@hku.hk

<sup>1</sup> College of Civil Engineering, Hunan University of Technology, Zhuzhou, China

<sup>2</sup> Department of Civil Engineering, The University of Hong Kong, Pokfulam, Hong Kong

method, rubber size, rubber content and confining pressure. Edil and Bosscher [16] studied the strength, compressibility and permeability characteristics of tire chips and soil mixtures using direct shear tests, compression tests and water pressure tests. They reported on the potential of the mixtures as a lightweight drainage material in highway and landfill construction. Foose et al. [20] conducted large-scale direct shear tests on sand reinforced with shredded waste tires, considering the influences of rubber content, normal stress, shred length, and shred orientation on shear strength. To discuss and evaluate the feasibility of using the mixtures as cost-effective substitutes for geotechnical fillings, Wu et al. [60] performed triaxial compression tests following stress paths on tire chips with rubber sizes of 2–38 mm and studied the effects of gradation and particle shape on shear strength. Lee et al. [29] carried out consolidated drained triaxial tests on the mixtures of Ottawa soils and tire chips and proposed a nonlinear hyperbolic model of the mixtures based on the original Duncan model. Yang et al. [63] developed a series of laboratory static test methods considering the effects of rubber size (2–10 mm) and confining pressure. They found that the shear strength of shredded tires is independent of particle size and that the transverse strain ratio is independent of confining pressure. Zornberg et al. [67] investigated the influence of tire shred shape on the shear strength of tire shred-soil mixtures. Their experimental results indicated that the greater the length–width ratio of tire shred is, the greater the shear strength of the mixtures is. Rao and Dutta [45] studied the compressibility and strength behavior of sand-tire chip mixtures. Their results showed that the shear strength of the mixtures decrease with increasing rubber content, and the mixture with a mass ratio of 20% could be used as a low-cost filler for highway embankments. More follow-up studies, such as Senetakis et al. [48], Sellaf et al. [47], Kyser and Ravichandran. [26], Wu et al. [43], Benessalah et al. [8], Zhang et al. [65] and Dai et al. [12] amply demonstrated that the mechanical properties of the mixtures can be significantly improved by adjusting the contents of waste tires.

The works mentioned above mainly focused on the influence of various factors (e.g., rubber content, confining pressure, tire rubber shape, and specimen preparation method) on the engineering properties of various RSMs (including chip, shred, granulated) and accumulated valuable experience for applying RSMs in practical engineering. However, the addition of rubber will result in a reduction in the strength and modulus compared to pure sand. For example, the friction angle decreases with increasing rubber content [67], increasing the earth pressure on the retaining walls when used as an engineering filler and reducing the bearing capacity when used as a foundation cushion. In this regard, it is believed that the

introduction of geogrid to reinforce RSM may be an effective option. The frictional locking effect between the geogrid and granulated sand can improve the shear strength of RSM, thereby enhancing the bearing capacity of the weak foundation and the overall stability of the superstructure. The reinforcement effect of geogrid on ordinary soils has already been extensively studied (e.g., see [10, 21, 33, 40, 54, 56]). However, to the best of our knowledge, research on the stress–strain–strength behavior of geogrid-reinforced RSM is still very limited.

In this study, a series of consolidated drained triaxial tests were conducted to investigate the effect of the reinforcement layer (one to three layers), rubber content (0–40%) and confining pressure (50 kPa, 100 kPa, and 200 kPa) on the stress–strain response and strength parameters (including peak strength, effective cohesion and effective friction angle) of granulated RSM, and a new equation for estimating the strength reinforcement effect of the composite mixtures is proposed. This paper discusses the reinforcement mechanism of geogrid on RSM, which is conducive to the implementation of more rational reuse of waste tire rubber and the subsequent research on the application of RSM to geotechnical and earthquake engineering.

## 2 Experimental program

### 2.1 Materials used

The sand used in the test is ISO standard sand from Xiamen, Fujian province, China, and it was purchased from Xiamen Aisiou Co., Ltd. The grain size of used sand varied between 0.05 and 2.0 mm, and its distribution curve is shown in Fig. 1. The specific gravity of the sand is 2.65, estimated as per ASTM D854 [5]. The sand is classified as

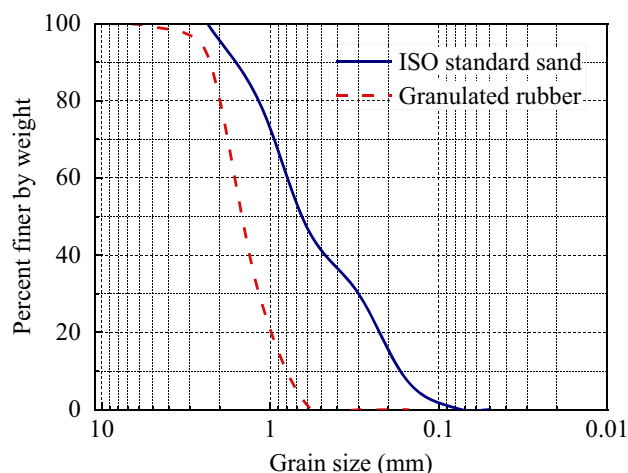


Fig. 1 Particle size distribution curves of the test materials

**Table 1** Physical properties of China ISO standard sand and granulated rubber

Test material	Description	Value
ISO standard sand	Mean size, $D_{50}$	0.64 mm
	Uniformity coefficient ( $C_u$ )	2.23
	Specific gravity ( $G_s$ )	2.65
	Maximum dry density	1.86 g/cm <sup>3</sup>
	Minimum dry density	1.51 g/cm <sup>3</sup>
	Maximum void ratio ( $e_{max}$ )	0.91
	Minimum void ratio ( $e_{min}$ )	0.58
Granulated rubber	Mean size, $D_{50}$	1.51 mm
	Uniformity coefficient ( $C_u$ )	4.77
	Specific gravity ( $G_s$ )	1.21
	Bulk density	0.51 g/cm <sup>3</sup>

poorly graded sand according to the unified classification system (UCS), ASTM-D2487 [3]. Other details of sand are presented in Table 1.

The rubber was procured from a local rubber processing factory and was classified as granulated rubber. It consists of scrap tires from which the steel and fibers have been removed. As per ASTM D6270 [4], particulate rubber composed of non-spherical particles with size ranges from 425 to 12 mm is referred to as granulated rubber. The grain size of used granulated rubber varied between 0.5 and 5.0 mm, and its distribution curve is shown in Fig. 1. The bulk density of granulated rubber is based on standard compaction test procedure, estimated as per ASTM D7481–18 [7]. Other details of granulated rubber are presented in Table 1.

The geosynthetic material used in the present study was a bidirectional geogrid made of glass fiber. Its mechanical properties (provided by the manufacturer) are presented in Table 2. The test equipment was a strain-controlled triaxial apparatus, consisting of a triaxial chamber, pressure control and axial loading devices, which was equipped with volume change and axial deformation measurement devices. Typical photos of the material samples and bidirectional geogrid used in the present study are shown in Fig. 2.

Granulated rubber was mixed with sand in a certain proportion, in which the rubber content by weight is

defined as the ratio of the weight of the rubber to total weight of the specimen. To ensure the comparability of the test results, the same relative density of 0.7 was adopted for RSM specimens with different rubber contents (0%, 10%, 20%, 30% and 40%). In this test, three types of geogrid arrangements were considered, namely, no reinforcement, 1-layer reinforcement, 2-layer reinforcement and 3-layer reinforcement.

## 2.2 Sample preparation and testing procedure

The specimen is cylindrical, with a size of 61.8 mm in diameter and 125 mm in height, and was prepared by moist compaction. Geosynthetics were arranged in horizontal layers as this increases strength, mainly through friction, and interlocking between the grains and the reinforcement. The mixtures were spooned into a metal mold to form 6 or 8 layers, and each layer was processed to a suitable height using the undercompaction method [27]. More specifically, 6-layer specimen holds for 1-layer and 2-layer reinforcement, and 8-layers specimen holds for 3-layer reinforcement. To avoid separation during sample preparation, the RSM was mixed uniformly in layers beforehand and then transferred into the molds. At each layer of the cylindrical specimen, it is gently compacted through a metal disc whose diameter was slightly smaller than the diameter of the mold. When reaching the predetermined horizontal layer, the precut geogrid was placed, followed by the filling of the upper later of RSM. Compared to unreinforced specimens, the interlayer spacing of the reinforced ones was kept constant and the number of RSM layers was adjusted to match the position of the reinforcement. The diameter of the geogrid layer was 1 ~ 3 mm less than that of the specimen to avoid edge effects, similar preparation procedures could refer to related studies, see Indraratna et al. [24] and Latha and Am [28].

To investigate the effects of the reinforcement (one to three layers), rubber content (0–40%) and confining pressure (50 kPa, 100 kPa, and 200 kPa) on the shear strength of RSM, a total of 60 consolidated drained (CD) triaxial compression tests were performed according to ASTM D7181 [6]. The prepared specimens were consolidated for 40 min under the target confining pressure and then tested at a loading rate of 0.32 mm/min.

**Table 2** Mechanical properties of the geogrid material

Material	Elongation (%)	Grid size (mm)	Elastic modulus (GPa)	Tensile strength (kN/m)	
				Longitudinal	Transversal
Glass fiber	≤ 3	12.7 × 12.7	67	60	60

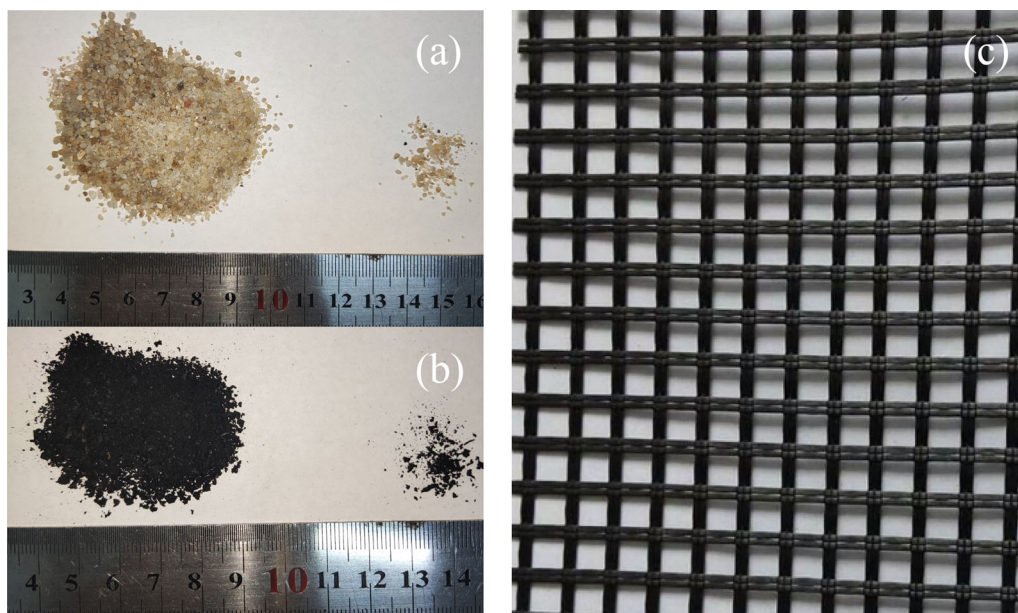


Fig. 2 Typical photos of test materials: **a** China ISO sand; **b** granulated rubber; and **c** bidirectional geogrid

### 3 Experimental results

#### 3.1 Stress–strain behavior

Figure 3 shows the stress–strain curves obtained from triaxial tests of unreinforced and reinforced RSMs (i.e., RSM and GGRSM) for a confining pressure of 100 kPa with varying percentages of rubber. The effects of the rubber content and reinforcement layers can be noticed by significant changes in stress–strain behavior. At relatively low rubber contents, the stress–strain curves exhibit the typical dilatancy and softening characteristics for the unreinforced RSM. The mechanical properties of RSM at a lower percentage of rubber tended toward that of pure sand with dense sand behavior due to dominant rigid sand–sand particle contact [61]. However, as the percentage of rubber increased to 30% and 40%, the softening characteristics of the stress–strain curve of the unreinforced RSM gradually vanished. This demonstrates that as the granulated rubber increases, the rigid sand–sand contact in the mixture is displaced by the flexible rubber–sand and rubber–rubber contacts. Granulated rubber with strong elastic deformation ability can be regarded as an equivalent void [55], causing pure sand to exhibit a loose sand behavior [62]. The geogrid inhibited the softening characteristics of the stress–strain curve for the lower percentage of rubber and improved the peak and residual strength. The hardening characteristics of the stress–strain curve for higher percentages of rubber were improved by the geogrid, and both the initial modulus and peak strength increased.

Furthermore, with an increasing number of reinforcement layers, the stress–strain curves of GGRSM rose significantly.

Generally, the stress–strain relationships for both RSM and GGRSM exhibited hardening or softening characteristics under different test conditions, with typical hyperbolic forms. Thus, the Duncan–Chang hyperbolic model can be employed to describe the presented stress–strain curves presented [15]:

$$\sigma_1 - \sigma_3 = \frac{E_0 \varepsilon_1}{1 + (\varepsilon_1 / \varepsilon_r)^\alpha} \quad (1)$$

where  $\sigma_1$  is the axial stress;  $\sigma_3$  is the confining pressure;  $E_0$  is the initial elastic modulus;  $\varepsilon_1$  is the axial strain;  $\varepsilon_r$  is the reference axial strain; and  $\alpha$  is the exponential parameter of the Duncan–Chang model. Using Eq. (1) to fit the stress–strain response, the obtained fitted curves are plotted in Fig. 3b–f (solid lines in the subfigures). It is evident that the experimental data can be fitted well.

Moreover, to validate the correctness of the experiments in the present study, Fig. 4 presents the comparison of the Duncan–Chang model’s parameters from the unreinforced results of the present study and previous studies (see [23, 66]). The relationships between the initial elastic modulus and reference strain of RSM with different rubber contents are in good agreement with the results of previous studies, which proves the reliability of the presented results to a certain extent.

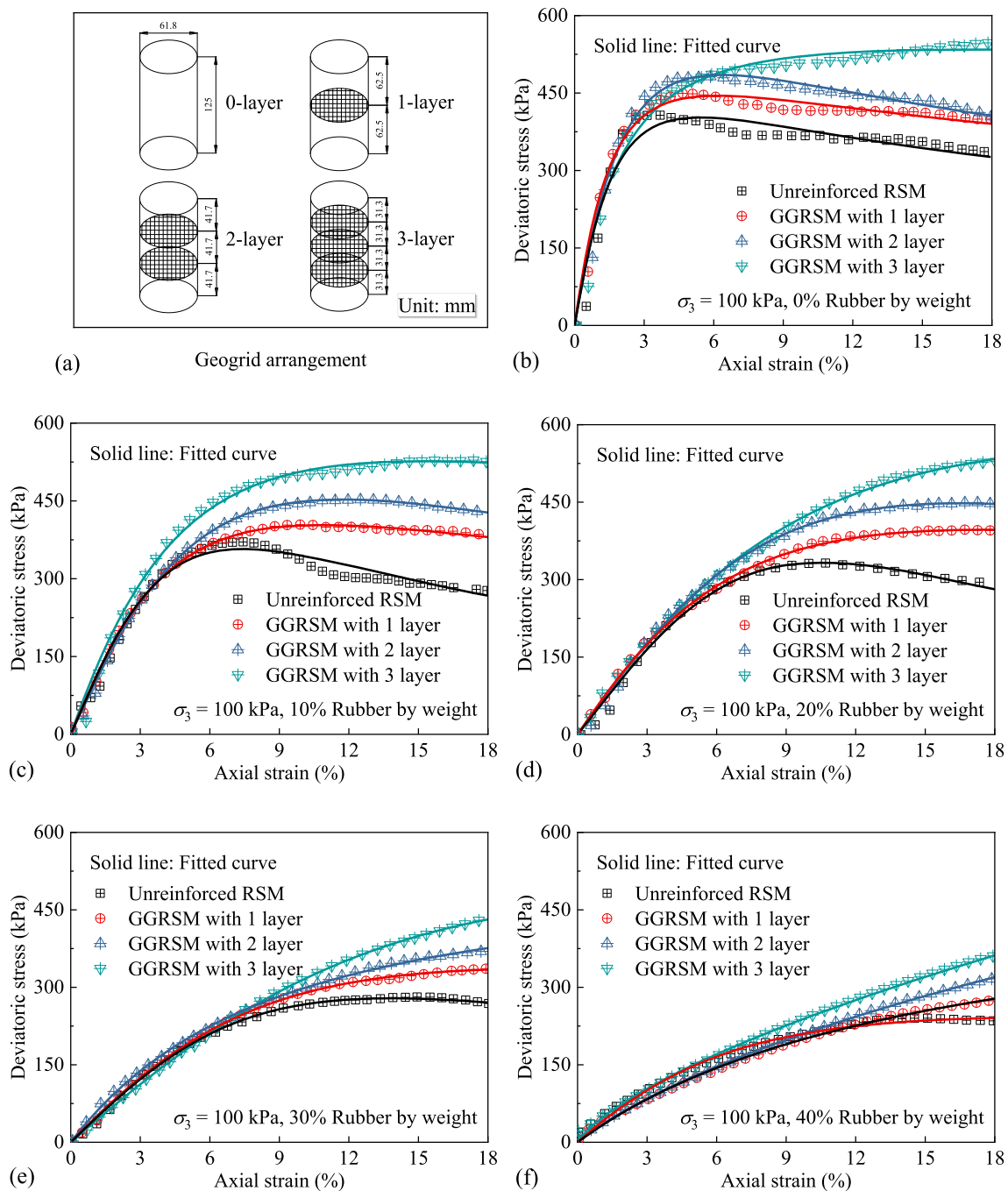


**Fig. 3** Stress–strain curves of the unreinforced and reinforced specimens (i.e., RSM and GGRSM) for a confining pressure of 100 kPa with different percentages of rubber: **a** details of the specimens; **b** rubber content of 0%; **c** rubber content of 10%; **d** rubber content of 20%; **e** rubber content of 30%; and **f** rubber content of 40%

### 3.2 Shear strength

Based on the obtained test results, the peak strength was determined as follows. If there was a peak value in the stress–strain curve, the peak deviatoric stress was taken. If there was no peak in the stress–strain curve, the deviatoric stress at the axial strain of 15% was taken. As a result, the

strength parameters of RSM and GGRSM with different percentages of rubber could be obtained.

Figure 5 shows the variations in the effective values of the peak strength  $q'_p$ , apparent cohesion  $c'$  and friction angle  $\varphi'$  of the unreinforced RSM with varying rubber contents, which were accompanied by the comparisons with the results of previous studies [1, 13, 18]. One can find

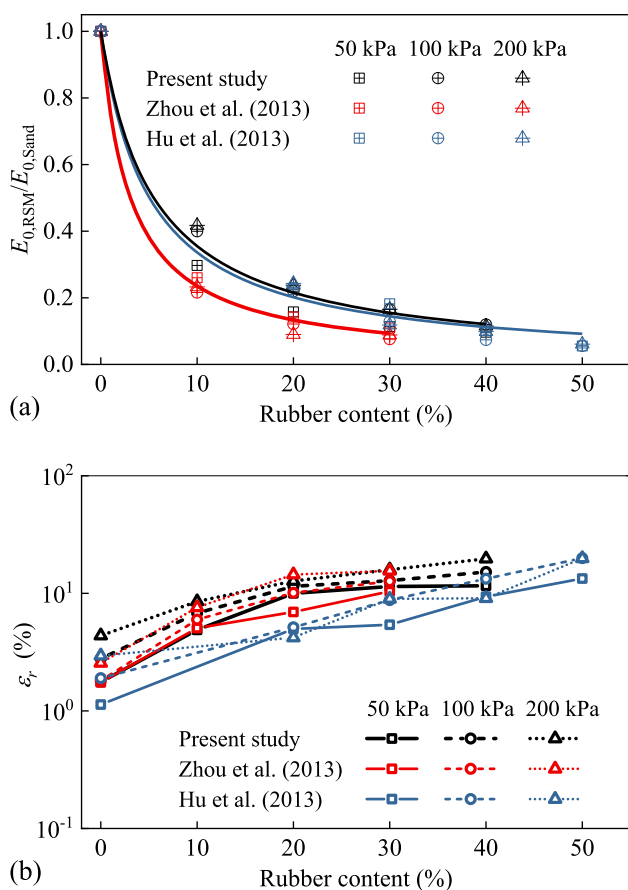


**Fig. 4** Comparison of the Duncan-Chang model parameters from the unreinforced results of the present study and previous studies: **a** initial elastic modulus and **b** axial strain

that  $q'_p$  decreased with increasing rubber content, and the greater the confining pressure is, the more pronounced the decrease;  $c'$  increased first and then decreased with increasing rubber content, generally reaching a maximum of 20% RSM; and  $\phi'$  decreased monotonically with increasing rubber content.

Figure 6 depicts the variations in the effective values of the peak strength of RSM and GGRSM with the rubber content at different confining pressures. The peak strengths of reinforced RSM were notably higher than those of the unreinforced one, and increased with an increasing number of reinforced layers. This is explained by the fact that with more layers and fewer arrangement intervals, the granular material between the horizontal reinforcement layers was more constrained, resulting in an increase in the peak strength of the specimen. Moreover, the peak strengths of GGRSM also decreased with increasing rubber content, and the decreasing rate of the peak strength of the reinforced specimen was more significant than that of the unreinforced one when the rubber content was less than

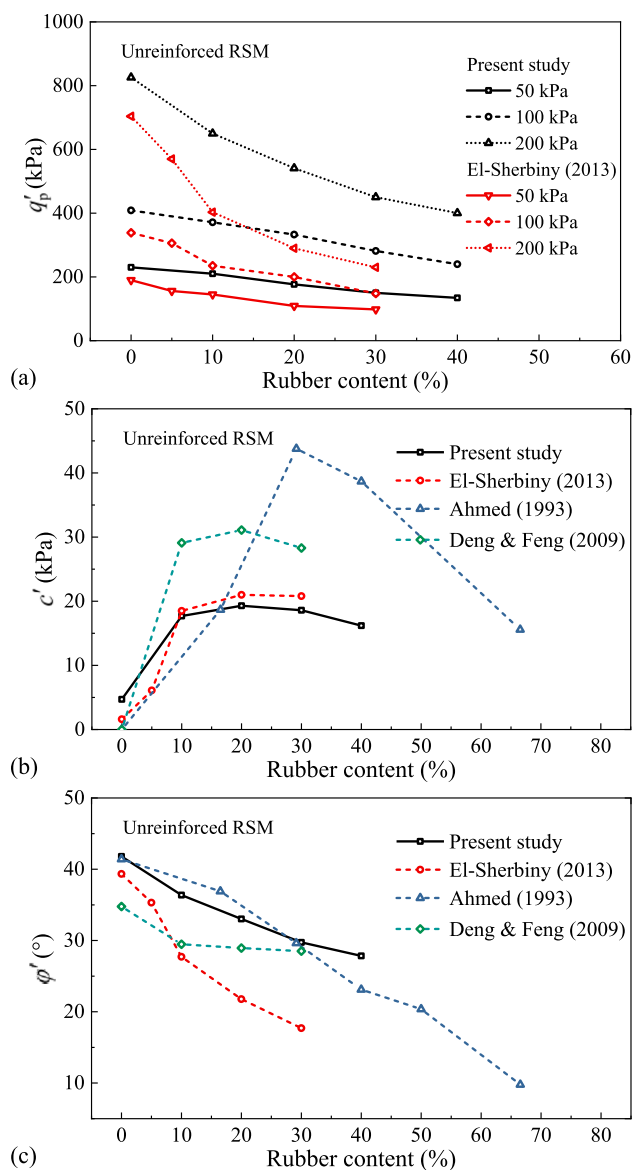


**Fig. 5** Variations in the effective values of the **a** peak strength, **b** apparent cohesion and **c** friction angle of RSM versus the rubber content

20%. When the rubber content exceeded 20%, the peak strength curves have a double folded shape, and this decreasing pattern was more evident in the cases of multilayered reinforcement.

The above analysis demonstrates that although the obtained curves from the present and previous studies did not completely overlap due to the differences in the type of sand and rubber, test methods and test programs, the results of the rubber content influence on the strength characteristics from different tests were similar. Obviously, the comparison of the results presented in this subsection further validates the reliability of the presented triaxial

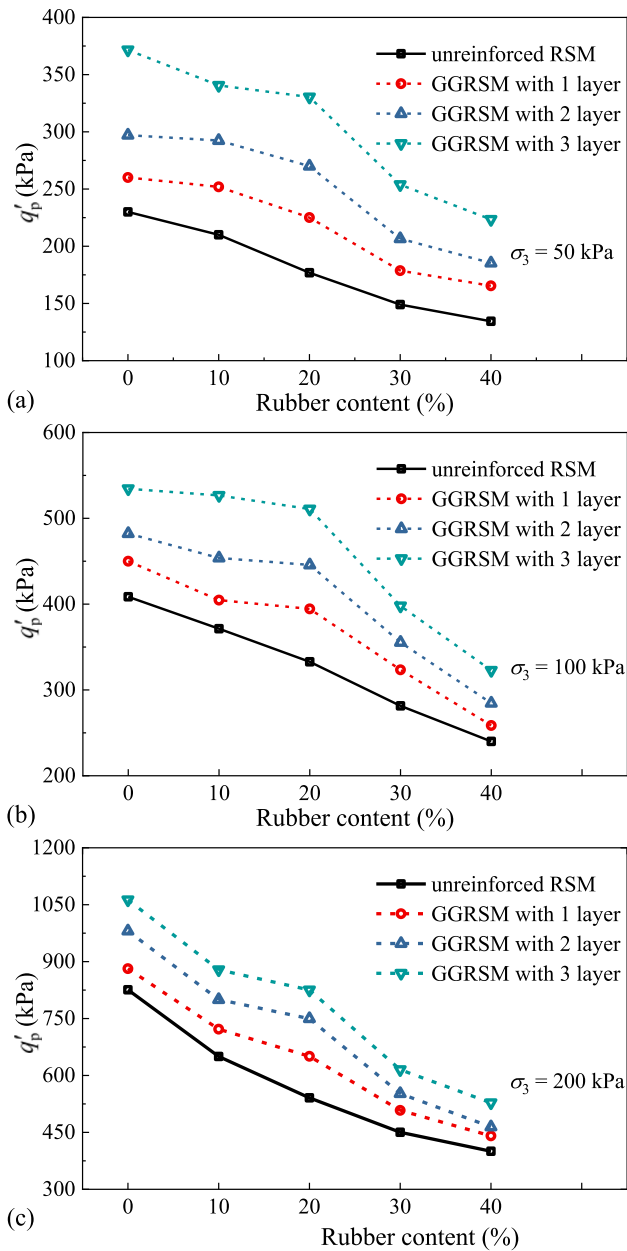


**Fig. 6** Variations in the effective values of the peak strength of RSM and GGRSM versus the rubber content at different confining pressures of **a** 50 kPa, **b** 100 kPa and **c** 200 kPa

compression tests and confirm that reinforcement is necessary due to the reduced strength of pure sand caused by the addition of rubber.

### 3.3 Quantitative analysis of reinforcement effect

Taking the confining pressure of 100 kPa as an example, the variations in the effective values of the peak strength, apparent cohesion and friction angle with the number of reinforcement layers for different percentages of rubber are shown in Fig. 7. These results indicate that the strength

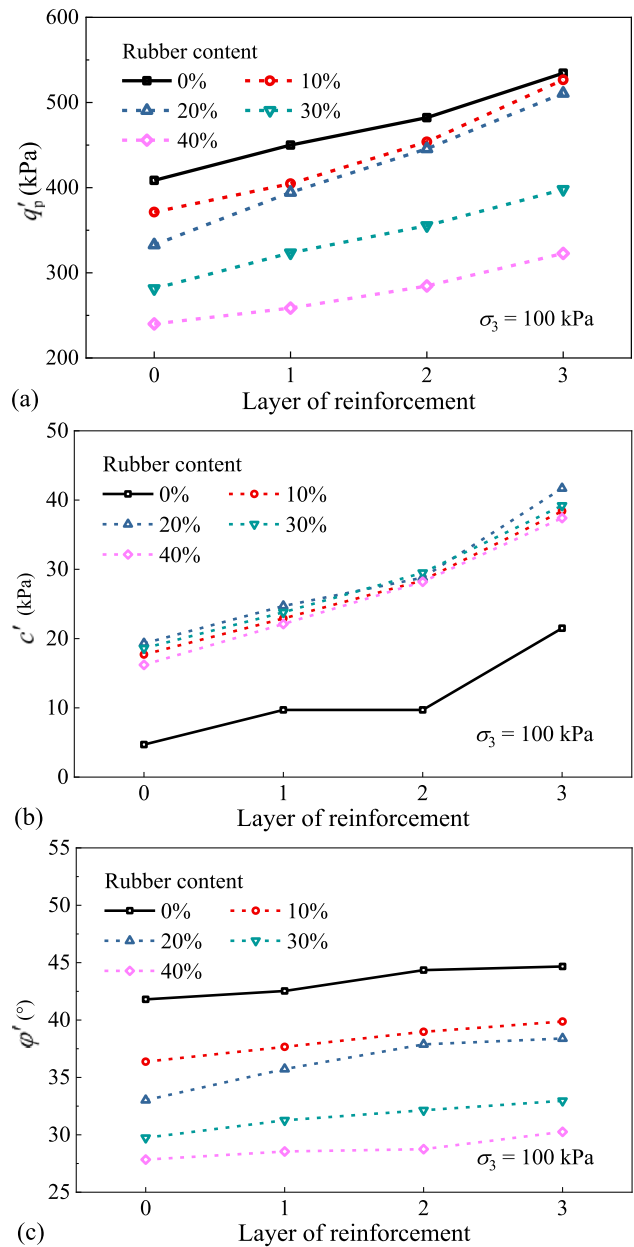


**Fig. 7** Variations in the effective values of the **a** peak strength, **b** apparent cohesion and **c** friction angle with the number of reinforcement layers

parameters of GGRSM increased approximately linearly with the number of reinforcement layers. To quantitatively describe the influence of geogrid reinforcement on shear strength, the reinforcement effect coefficients are introduced by

$$R_q = \frac{q'_{p,GGRSM}}{q'_{p,RSM}} \quad (2)$$

$$R_{c'} = \frac{c'_{\text{GGRSM}}}{c'_{\text{RSM}}} \quad (3)$$

$$R_{\phi'} = \frac{\phi'_{\text{GGRSM}}}{\phi'_{\text{RSM}}} \quad (4)$$

where  $R_{q'}$ ,  $R_{c'}$  and  $R_{\phi'}$  are the reinforcement coefficients for the effective values of the peak strength, apparent cohesion and friction angle, respectively.

Simultaneously, the reinforcement density is introduced to quantitatively characterize different reinforcement layers:

$$\rho_R = \frac{nB}{H} \quad (5)$$

where  $\rho_R$  is the reinforcement density;  $B$  is the width of the specimen (i.e., the cross-sectional diameter for triaxial tests);  $H$  is the height of the specimen; and  $n$  is the number of reinforcement layers.

Figure 8 shows the relationships of the reinforcement coefficients for the effective values of the peak strength of GGRSM with the rubber content. Overall,  $R_{q'}$  increased first and then decreased and reached its maximum at 20% of rubber inclusions. For the same rubber contents, the lower the confining pressure and the greater the number of geogrid layers, the stronger the strength reinforcement effect. Figure 9 plots the relationships of the reinforcement coefficients for the effective apparent cohesion and effective friction angle of GGRSM with the rubber content. In presented results, all  $R_{c'}$  and  $R_{\phi'}$  were greater than 1.0, which indicates that geogrid reinforcement can improve the shear strength, and the reinforcement effect is more obvious with more layers. For  $R_{c'}$ , the effect of geogrid reinforcement on the effective apparent cohesion of pure sand was the greatest, even though it had little effect on RSM. For  $R_{\phi'}$ , the reinforcement effect was significantly influenced by the rubber content, showing a hump-shaped trend

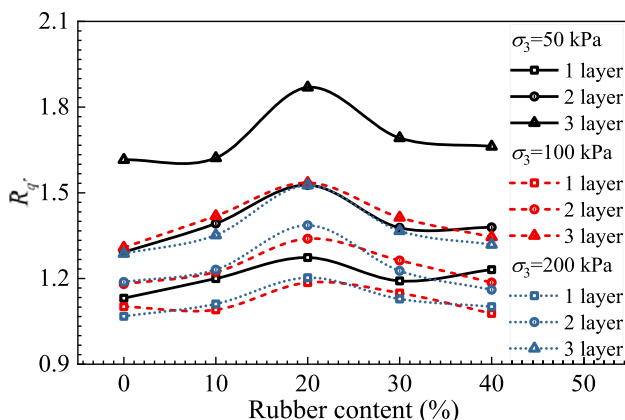


**Fig. 8** Variations the reinforcement coefficients for the effective values of the peak strength of GGRSM versus the rubber content

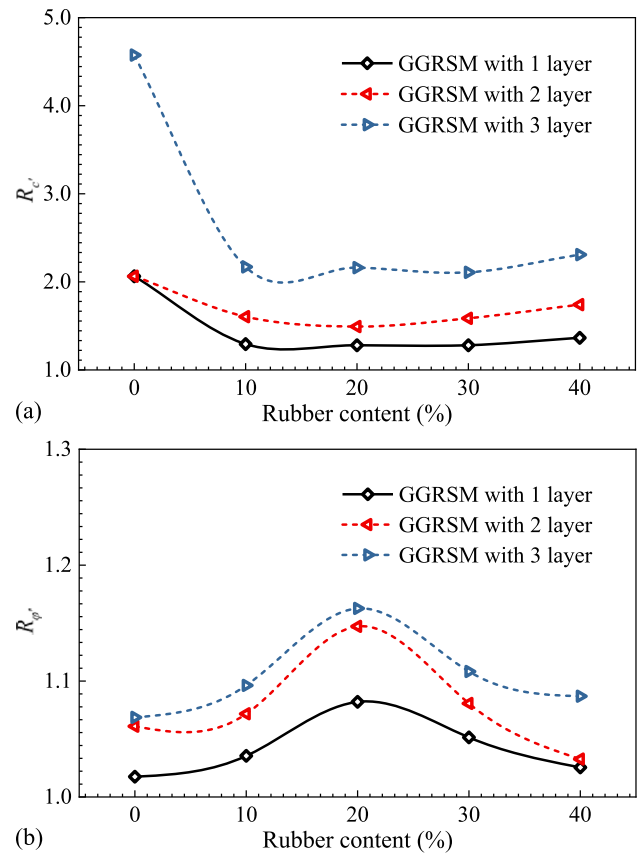


**Fig. 9** Variations in the reinforcement coefficients for the **a** effective apparent cohesion and **b** effective friction angle of GGRSM versus the rubber content

of increasing and then decreasing, in which RSM with 20% rubber content was probably optimal.

Figure 10 compares the strength reinforcement coefficient versus the reinforcement density obtained in the present study and in Peng et al. [42], where the effects of the number of reinforcement layers and the rubber content are shown in Fig. 10a and b, respectively. Both the results presented in this paper and the publications reveal that the strength reinforcement coefficient of the reinforced specimens increased with increasing reinforcement density. For lower confining pressures (19.6 kPa in Peng's work and 50 kPa in the present study), the slopes of the latter parts of the  $R_{q'} \sim \rho_R$  curves increased dramatically, indicating that the reinforcement effect increases at an accelerated rate with increasing reinforcement density. Although the slopes of the  $R_{q'} \sim \rho_R$  curves obtained from the two tests are quite different due to the differences in test materials, test methods and confining pressures, the resulting patterns are still similar.

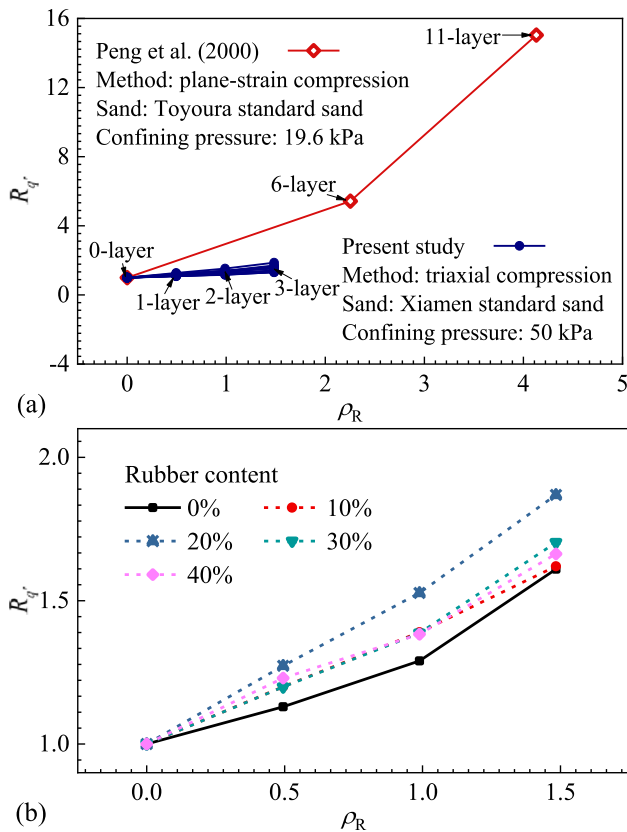


**Fig. 10** Relationship between the strength reinforcement coefficient and the reinforcement density: **a** the effect of the number of reinforcement layers and **b** the effect of rubber content

#### 4 Discussion and future work

The reinforcement mechanism of geogrid with granular materials can be attributed to two effects, one being the friction between the grid and the granular material and the other being the bite force generated by the grid against the lateral displacement of granular material. This limits the lateral expansion deformation and improves the average shear strength of the medium in the local range. With increasing reinforcement density (more layers and a closer arrangement), the restricted local area increases. Thus, the average shear strength of the medium is further improved, and the reinforcement effect is more significant on the macro level.

For RSM, the higher the granulated rubber content is, the greater the proportion of sand–rubber and rubber–rubber contacts in the force transfer skeleton of RSM. For lower confining pressures, the lateral deformation trend of reinforced RSM in the triaxial test become more pronounced, and the reinforcement effect of the geogrid is more fully exploited. Actually, the confining pressure in the work of Peng et al. [42] is lower than that in the present study, and the corresponding slopes of the  $R_{\sigma} \sim \rho_R$  curves

are steeper, which is also an indication of the reinforcement mechanism. Furthermore, a rubber content of 20% for reinforced specimen might be an optimal value from the perspective of material stability. At around this percentage, the shear strength and overall stability of the composite mixtures are superior to that of pure sand. In the prevailing mechanism, granulated rubber in the mixture plays an integrated role due to its low modulus and strong deformability [57]. More specifically, the strong contact force chains of RSM specimen with such rubber content would increase monotonically with axial strain, and the stress–strain curves would form a relatively stable strain-hardening characteristic with small volume shrinkage. As also reported in previous studies such as Mashiri et al. [37], Liu et al. [30], Khatami et al. [25], the shear stiffness resulting from a reasonable level of rubber inclusion could meet the engineering requirements, in this case the mixture features a higher damping ratio and better energy dissipation.

Overall, reinforcement of RSM with geosynthetics possess many potential benefits in geotechnical and earthquake engineering applications. Reinforced RSM could be better used as a fill material to reduce the contact pressure with the underlying soil and the deformation of facing [14, 32, 59]. Also, RSM as foundation material provides an available and low-cost solution for seismic isolation, while the use of reinforcement is capable of overcoming the shortcomings of RSM in terms of shear resistance and bearing capacity [2, 17, 19, 36]. In the present study, a number of well-designed and executed triaxial compression tests have been performed to evaluate the stress–strain–strength behavior of reinforced RSMs. Nevertheless, all conclusions regarding geosynthetic reinforcement may be constrained by the specimen size, effective openings, geogrid materials and boundary effects [21, 22, 28, 33]. To further evaluate the use of geosynthetics to enhance RSM, large size geotechnical testing and numerical analysis are required.

Our future work will focus on the monotonic and cyclic behaviors of the reinforced RSM–structure interface through large-scale pull-out tests and large-scale simple shear tests (see Fig. 11). In this regard, the influence of the varying factors such as grain size and shape, rubber content, relative density, contact surface roughness, and normal stress would be considered, and then a geosynthetics–RSM–structure mechanical model would be developed to determine the statics/dynamic contact parameters. On the other side, 3D discrete element numerical simulations would be carried out to investigate the macro- and micro-mechanisms of key factors on the stress–strain–strength of geosynthetic RSM. Actually, previous studies have shown a direct correlation between bulk friction and microscopic friction for sand–rubber composites (e.g., see [31, 35, 51].

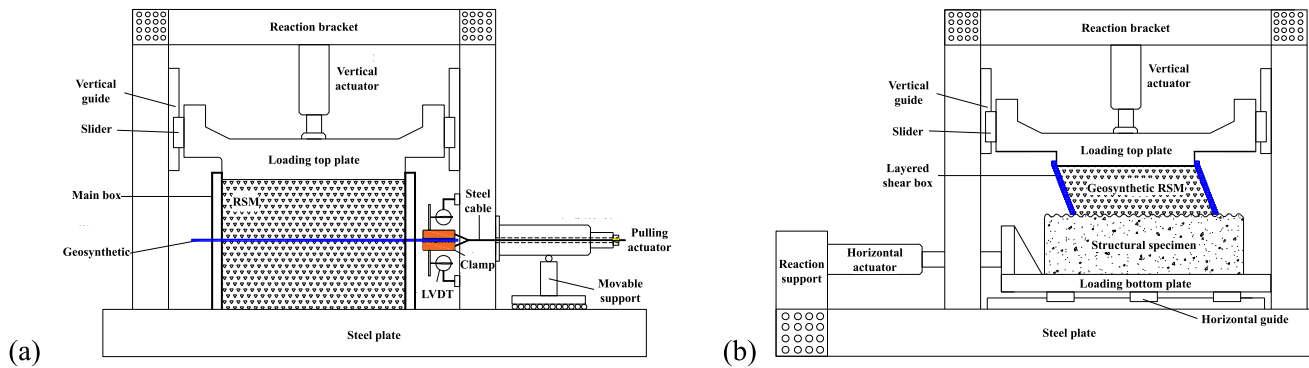


**Fig. 11** Planning scheme of large-scale geotechnical tests for geosynthetic RSM through **a** pull-out apparatus and **b** simple shear apparatus

As can be expected, the geogrid-mixture interface during the shearing process would result in large deformed strip, violent particle movement and interesting contact force distribution. With the experimental finding and mechanism analysis, the optimized proportioning parameters of geosynthetic RSM applicable to geotechnical engineering and earthquake resistant design could finally be proposed.

## 5 Conclusion

In this study, the stress–strain–strength behaviors of geosynthetic-reinforced RSM were investigated through a series of triaxial tests, and the effects of the rubber contents (0%, 10%, 20%, 30% and 40%), reinforcement schemes (one-, two- and three-layer geogrid arrangements) and confining pressures (50 kPa, 100 kPa and 200 kPa) on the shear strength parameters were evaluated and discussed. Based on the test results, the following conclusions can be drawn:

1. The strength parameters of the geogrid-reinforced RSM, including the effective values of peak strength, apparent cohesion and friction angle, were significantly improved compared to those of the unreinforced RSM. The improvement effect increased with the increase in the number of reinforcement layers and decreased with the increase in confining pressure.
2. With increasing rubber content, the reinforcement coefficient for effective apparent cohesion decreased rapidly at first and then tended to become stable, while the reinforcement coefficients for effective friction angle and peak strength increased first and then decreased. When the rubber content was 20%, all shear strength parameters might be the optimal.
3. A comparison between this work and the previous studies suggests, the strength reinforcement coefficient of the geosynthetic granular sand/sand-rubber would be

increased with increasing reinforcement density, especially for the low confining pressure cases.

Additionally, further research on the macro- and micro-mechanical properties of reinforced RSM using advanced geotechnical tests, discrete element modeling, and large-scale field evaluations is recommended to reasonably determine the optimized proportioning parameters of geosynthetic composite mixtures for applications in different engineering projects.

**Acknowledgements** The authors are grateful for the financial supports provided by the Research Fund of Institute of Engineering Mechanics, China Earthquake Administration under Grant no. 2019D25, the Natural Science Foundation of Hunan Province under Grant no. 2020JJ6073, the Key Research Project of Hunan Provincial Department of Education under Grant no. 21A0357, and the Postdoctoral Foundation of the University of Hong Kong. Many thanks to the anonymous reviewers for their comprehensive and detailed comments on the original manuscript.

**Data availability** The datasets generated during and analyzed during the current study are available from the corresponding author on reasonable request.

## Declarations

**Conflict of interest** The authors have no relevant financial or non-financial interests to disclose.

## References

1. Ahmed I (1993) Laboratory study on properties of rubber-soils, Doctoral dissertation, Purdue University.
2. Liu FC, Wu MT, Liu N, Zhang YF, Chen JL (2017) Experimental study on Poisson's ratio of rubber-sand mixtures. *Chin J Rock Mech Eng* 36(S1):3596–3606. <https://doi.org/10.13722/j.cnki.jrme.2016.0590>
3. ASTM (2003) Standard practice for classification of soils for engineering purposes. Unified Soil Classification System. ASTM D2487
4. ASTM (2008) Standard practise for use of scrap tires in civil engineering applications. ASTM D6270

5. ASTM (2010) Standard test methods for specific gravity of soils by water pycnometer. ASTM D854
6. ASTM (2011) Standard method for consolidated drained triaxial compression test for soils. ASTM D7181
7. ASTM (2018) Standard test methods for determining loose and tapped bulk densities of powders using a graduated cylinder. ASTM D7481–18
8. Benessalah I, Arab A, Sadek M, Bouferra R (2019) Laboratory study on the compressibility of sand–rubber mixtures under one dimensional consolidation loading conditions. *Granular Matter* 21(1):7. <https://doi.org/10.1007/s10035-018-0860-8>
9. Christ M, Park JB, Hong SS (2010) Laboratory observation of the response of a buried pipeline to freezing rubber-sand backfill. *J Mater Civ Eng* 22(9):943–950. [https://doi.org/10.1061/\(ASCE\)MT.1943-5533.0000090](https://doi.org/10.1061/(ASCE)MT.1943-5533.0000090)
10. Correia NS, Zornberg JG (2018) Strain distribution along geogrid-reinforced asphalt overlays under traffic loading. *Geotext Geomembr* 46(1):111–120. <https://doi.org/10.1016/j.geotextmem.2017.10.002>
11. Cui MJ, Zheng JJ, Dahal BK, Lai HJ, Huang ZF, Wu CC (2021) Effect of waste rubber particles on the shear behaviour of biocemented calcareous sand. *Acta Geotech* 16(5):1429–1439. <https://doi.org/10.1007/s11440-021-01176-y>
12. Dai BB, Liu Q, Mao X, Li PY, Liang ZZ (2023) A reinterpretation of the mechanical behavior of rubber-sand mixtures in direct shear testing. *Constr Build Mater* 363:129771. <https://doi.org/10.1016/j.conbuildmat.2022.129771>
13. Deng A, Feng JR (2009) Granular lightweight fill composed of sand and tire scrap. In: *Characterization, modeling, and performance of geomaterials: selected papers from the 2009 GeoHunan international conference*. pp 78–85. [https://doi.org/10.1061/41041\(348\)12](https://doi.org/10.1061/41041(348)12)
14. Manohar DR, Anbazhagan P (2021) Shear strength characteristics of geosynthetic reinforced rubber-sand mixtures. *Geotext Geomembr* 49(4):910–920. <https://doi.org/10.1016/j.geotextmem.2020.12.015>
15. Duncan JM, Chang CY (1970) Nonlinear analysis of stress and strain in soils. *J Soil Mech Found Div* 96(5):1629–1653. <https://doi.org/10.1061/JSFEAQ.0001458>
16. Edil TB, Bosscher PJ (1994) Engineering properties of tire chips and soil mixtures. *Geotech Test J* 17(4):453–464. <https://doi.org/10.1520/GTJ10306J>
17. Edinçliler A, Yildiz O (2022) Effects of processing type on shear modulus and damping ratio of waste tire-sand mixtures. *Geosynth Int*. <https://doi.org/10.1680/jgein.21.00008a>
18. El-Sherbiny R, Youssef A, Lotfy H (2013) Triaxial testing on saturated mixtures of sand and granulated rubber. In: *Geo-Congress 2013: stability and performance of slopes and embankments III*. pp 82–91. <https://doi.org/10.1061/9780784412787.009>
19. Fonseca J, Riaz A, Bernal-Sanchez J, Barreto Gonzalez D, McDougall J, Miranda Manzanares M, Dimitriadi V (2019) Particle-scale interaction in sand-rubber mixtures and their influence on energy dissipation mechanisms. *Géotech Lett* 9(4):1–6. <https://doi.org/10.1680/jgele.18.00221>
20. Foote GJ, Benson CH, Bosscher PJ (1996) Sand reinforced with shredded waste tires. *J Geotech Eng* 122(9):760–767. [https://doi.org/10.1061/\(ASCE\)0733-9410\(1996\)122:9\(760\)](https://doi.org/10.1061/(ASCE)0733-9410(1996)122:9(760))
21. Han B, Ling J, Shu X, Song W, Boudreau RL, Hu W, Huang B (2019) Quantifying the effects of geogrid reinforcement in unbound granular base. *Geotext Geomembr* 47(3):369–376. <https://doi.org/10.1016/j.geotextmem.2019.01.009>
22. Hang L, Gao Y, He J, Li C, Zhou Y, van Paassen LA (2022) Pullout behavior of biocement–geosynthetic reinforcement system: a parametric study. *Acta Geotech* 17(12):5429–5439. <https://doi.org/10.1007/s11440-022-01687-2>
23. Hu YC, Shen JM, Zhao JB, Gu GD, Cai HN (2013) Experimental study of engineering properties of geogrid-reinforced loess mixed with sand. *Rock Soil Mech* 34(2):74–81. <https://doi.org/10.16285/j.rsm.2013.s2.041>
24. Indraratna B, Ngo NT, Rujikiatkamjorn C (2011) Behavior of geogrid-reinforced ballast under various levels of fouling. *Geotext Geomembr* 29(3):313–322. <https://doi.org/10.1016/j.geotextmem.2011.01.015>
25. Khatami H, Deng A, Jaksa M (2020) The arching effect in rubber–sand mixtures. *Geosynth Int* 27(4):432–450. <https://doi.org/10.1680/jgein.20.00007>
26. Kyser D, Ravichandran N (2016) Properties of chipped rubber roofing membrane and sand mixtures for civil engineering applications. *J Build Eng* 7:103–113. <https://doi.org/10.1016/j.jobe.2016.05.008>
27. Ladd RS (1978) Preparing test specimens using undercompaction. *Geotech Test J* 1(1):16–23. <https://doi.org/10.1520/GTJ10364J>
28. Latha GM, Am NV (2016) Static and cyclic load response of reinforced sand through large triaxial tests. *Jpn Geotech Soc Spec Publ* 2(68):2342–2346. <https://doi.org/10.3208/jgssp.IGS-39>
29. Lee JH, Salgado R, Bernal A, Lovell CW (1999) Shredded tires and rubber-sand as lightweight backfill. *J Geotech Geoenviron Eng* 125(2):132–141. [https://doi.org/10.1061/\(ASCE\)1090-0241\(1999\)125:2\(132\)](https://doi.org/10.1061/(ASCE)1090-0241(1999)125:2(132))
30. Liu Q, Zhuang H, Wu Q, Zhao K, Chen G (2022) Experimental study on dynamic modulus and damping ratio of rubber–sand mixtures over a wide strain range. *J Earthq Tsunami* 16(2):2140006. <https://doi.org/10.1142/S1793431121400066>
31. Li W, Kwok CY, Sandeep CS, Senetakis K (2019) Sand type effect on the behaviour of sand-granulated rubber mixtures: integrated study from micro-to macro-scales. *Powder Technol* 342:907–916. <https://doi.org/10.1016/j.powtec.2018.10.025>
32. Liu FC, Wu MT, Jing LP (2019) Experimental study on the isolating performance of a new reinforced rubber-sand mixture composite cushion. *J Vib Shock* 38(22):184–197. <https://doi.org/10.13465/j.cnki.ivs.2019.22.026>
33. Liu FY, Ying MJ, Yuan GH, Wang J, Ni JF (2021) Particle shape effects on the cyclic shear behaviour of the soil–geogrid interface. *Geotext Geomembr* 49(4):991–1003. <https://doi.org/10.1016/j.geotextmem.2021.01.008>
34. Liu HS, Mead JL, Stacer RG (2000) Environmental effects of recycled rubber in light-fill applications. *Rubber Chem Technol* 73(3):551–564. <https://doi.org/10.5254/1.3547605>
35. Lopera Perez JC, Kwok CY, Senetakis K (2017) Investigation of the micro-mechanics of sand–rubber mixtures at very small strains. *Geosynth Int* 24(1):30–44. <https://doi.org/10.1680/jgein.16.00013>
36. Madhusudhan BR, Boominathan A, Banerjee S (2020) Cyclic simple shear response of sand–rubber tire chip mixtures. *Int J Geomech* 20(9):04020136. [https://doi.org/10.1061/\(ASCE\)GM.1943-5622.0001761](https://doi.org/10.1061/(ASCE)GM.1943-5622.0001761)
37. Mashiri MS, Vinod JS, Sheikh MN (2016) Liquefaction potential and dynamic properties of sand-tyre chip (STCh) mixtures. *Geotech Test J* 39(1):69–79. <https://doi.org/10.1520/GTJ20150031>
38. Mehrjardi GT, Tafreshi SM, Dawson AR (2015) Numerical analysis on buried pipes protected by combination of geocell reinforcement and rubber-soil mixture. *Int J Civ Eng* 13(2):90–104. <https://doi.org/10.1016/j.resconrec.2020.104679>
39. Mohajerani A, Burnett L, Smith JV, Markovski S, Rodwell G, Rahman MT, Maghool F (2020) Recycling waste rubber tyres in construction materials and associated environmental considerations: a review. *Resour Conserv Recycl* 155:104679. <https://doi.org/10.1016/j.resconrec.2020.104679>

40. Mousavi SH, Gabr MA, Borden RH (2017) Optimum location of geogrid reinforcement in unpaved road. *Can Geotech J* 54(7):1047–1054. <https://doi.org/10.1139/cgj-2016-0562>
41. Patil U, Valdes JR, Evans TM (2011) Swell mitigation with granulated tire rubber. *J Mater Civ Eng* 23(5):721–727. [https://doi.org/10.1061/\(asce\)mt.1943-5533.0000229](https://doi.org/10.1061/(asce)mt.1943-5533.0000229)
42. Peng F, Kotake N, Tatsuoka F, Hirakawa D, Tanaka T (2000) Plane strain compression behaviour of geogrid-reinforced sand and its numerical analysis. *Soils Found* 40(3):55–74. [https://doi.org/10.3208/sandf.40.3\\_55](https://doi.org/10.3208/sandf.40.3_55)
43. Wu MT, Liu FC, Chen JL, Chen L (2018) Influence of water content on dynamic shear modulus and damping ratio of rubber-sand mixture under large strains. *Rock Soil Mech* 39(3):803–814. <https://doi.org/10.16285/j.rsm.2017.0956>
44. Pitilakis K, Karapetrou S, Tsagdi K (2015) Numerical investigation of the seismic response of RC buildings on soil replaced with rubber–sand mixtures. *Soil Dyn Earthq Eng* 79:237–252. <https://doi.org/10.1016/j.soildyn.2015.09.018>
45. Rao GV, Dutta RK (2006) Compressibility and strength behaviour of sand–tyre chip mixtures. *Geotech Geol Eng* 24(3):711–724. <https://doi.org/10.1007/s10706-004-4006-x>
46. Reddy SB, Krishna AM (2015) Recycled tire chips mixed with sand as lightweight backfill material in retaining wall applications: an experimental investigation. *Int J Geosynth Ground Eng* 1(4):1–11. <https://doi.org/10.1007/s40891-015-0036-0>
47. Sellaf H, Trouzine H, Hamhami M, Asroun A (2014) Geotechnical properties of rubber tires and sediments mixtures. *Eng Technol Appl Sci Res* 4(2):618–624. <https://doi.org/10.5281/zenodo.14041>
48. Senetakis K, Anastasiadis A, Pitilakis K (2012) Dynamic properties of dry sand/rubber (SRM) and gravel/rubber (GRM) mixtures in a wide range of shearing strain amplitudes. *Soil Dyn Earthq Eng* 33(1):38–53. <https://doi.org/10.1016/j.soildyn.2011.10.003>
49. Soltani-Jigheh H, Asadzadeh M, Marefat V (2014) Effects of tire chips on shrinkage and cracking characteristics of cohesive soils. *Turk J Eng Environ Sci* 37(3):259–271. <https://doi.org/10.3906/kim-1208-19>
50. Tafreshi SM, Mehrjardi GT, Dawson AR (2012) Buried pipes in rubber-soil backfilled trenches under cyclic loading. *J Geotech Geoenviron Eng* 138(11):1346–1356. [https://doi.org/10.1061/\(ASCE\)GT.1943-5606.0000710](https://doi.org/10.1061/(ASCE)GT.1943-5606.0000710)
51. Tian Y, Senetakis K (2022) On the contact problem of soft-rigid interfaces: incorporation of Mindlin-Deresiewicz and self-deformation concepts. *Granular Matter* 24(1):1–17. <https://doi.org/10.1007/s10035-021-01186-3>
52. Tsang HH (2008) Seismic isolation by rubber–soil mixtures for developing countries. *Earthq Eng Struct Dyn* 37(2):283–303. <https://doi.org/10.1002/eqe.756>
53. Tweedie JJ, Humphrey DN, Sandford TC (1998) Tire shreds as lightweight retaining wall backfill: active conditions. *J Geotech Geoenviron Eng* 124(11):1061–1070. [https://doi.org/10.1061/\(ASCE\)1090-0241\(1998\)124:11\(1061\)](https://doi.org/10.1061/(ASCE)1090-0241(1998)124:11(1061))
54. Venkateswarlu H, Ujjawal KN, Hegde A (2018) Laboratory and numerical investigation of machine foundations reinforced with geogrids and geocells. *Geotext Geomembr* 46(6):882–896. <https://doi.org/10.1016/j.geotextmem.2018.08.006>
55. Verdugo R, Ishihara K (1996) The steady state of sandy soils. *Soils Found* 36(2):81–91. [https://doi.org/10.3208/sandf.36.2\\_81](https://doi.org/10.3208/sandf.36.2_81)
56. Wang JQ, Zhang LL, Xue JF, Tang Y (2018) Load-settlement response of shallow square footings on geogrid-reinforced sand under cyclic loading. *Geotext Geomembr* 46(5):586–596. <https://doi.org/10.1016/j.geotextmem.2018.04.009>
57. Wu M, Liu F, Li Z, Bu G (2022) Micromechanics of granulated rubber–soil mixtures as a cost-effective substitute for geotechnical fillings. *Mech Adv Mater Struct*. <https://doi.org/10.1080/15376494.2022.2062628>
58. Wu M, Tian W, Liu F, Yang J (2023a) Seismic isolation effect of rubber-sand mixture cushion under different site classes based on a simplified analysis model. *Soil Dyn Earthq Eng* 166:107738. <https://doi.org/10.1016/j.soildyn.2022.107738>
59. Wu M, Tian W, Liu F, Yang J (2023b) Dynamic behavior of geocell-reinforced rubber sand mixtures under cyclic simple shear loading. *Soil Dyn Earthq Eng* 164:107595. <https://doi.org/10.1016/j.soildyn.2022.107595>
60. Wu WY, Benda CC, Cauley RF (1997) Triaxial determination of shear strength of tire chips. *J Geotech Geoenviron Eng* 123(5):479–482. [https://doi.org/10.1061/\(ASCE\)1090-0241\(1997\)123:5\(479\)](https://doi.org/10.1061/(ASCE)1090-0241(1997)123:5(479))
61. Yang J, Liu X (2016) Shear wave velocity and stiffness of sand: the role of non-plastic fines. *Géotechnique* 66(6):1–15. <https://doi.org/10.1680/jgeot.15.P.205>
62. Yang J, Wei LM (2012) Collapse of loose sand with the addition of fines: the role of particle shape. *Géotechnique* 62(12):1111–1125. <https://doi.org/10.1680/geot.11.P.062>
63. Yang S, Lohnes RA, Kjartansson BH (2002) Mechanical properties of shredded tires. *Geotech Test J* 25(1):44–52. <https://doi.org/10.1520/GTJ11078J>
64. Yoon S, Prezzi M, Siddiki NZ, Kim B (2006) Construction of a test embankment using a sand–tire shred mixture as fill material. *Waste Manag* 26(9):1033–1044. <https://doi.org/10.1016/j.wasman.2005.10.009>
65. Zhang J, Chen X, Zhang J, Jitsangiam P, Wang X (2021) DEM investigation of macro-and micro-mechanical properties of rigid-grain and soft-chip mixtures. *Particology* 55:128–139. <https://doi.org/10.1016/j.partic.2020.06.002>
66. Zhou XF, Zhang MX, Qiu CC (2013) Strength of sand reinforced with different forms of geogrid. *J Shanghai Jiao Tong Univ* 47(9):1377–1381. <https://doi.org/10.16183/j.cnki.jsjtu.2013.09.009>
67. Zornberg JG, Cabral AR, Viratjandr C (2004) Behaviour of tire shred sand mixtures. *Can Geotech J* 41(2):227–241. <https://doi.org/10.1139/t03-086>

**Publisher's Note** Springer Nature remains neutral with regard to jurisdictional claims in published maps and institutional affiliations.

Springer Nature or its licensor (e.g. a society or other partner) holds exclusive rights to this article under a publishing agreement with the author(s) or other rightsholder(s); author self-archiving of the accepted manuscript version of this article is solely governed by the terms of such publishing agreement and applicable law.